Electronic Supplementary Information for "Broadening the energetic stability window of organic crystal polymorphs via solid-state synthetic memory"

Gregory J. O. Beran*

Department of Chemistry, University of California, Riverside, California 92521 USA

E-mail: gregory.beran@ucr.edu

Contents

S1 MP2D refinement

S1.1 Anthracene photodimerization benchmarks

The 9TBAE crystal energetics are refined here using the recently developed dispersion-corrected second-order Møller-Plesset perturbation theory (MP2D) model.[1] Benchmark coupled cluster singles, doubles, and perturbative triples (CCSD(T)) calculations demonstrate that the anthracene photodimerization reaction is exothermic, and the products are stable relative to isolated anthracenes (Figure S1).[1,2] In contrast, B86bPBE-XDM and many other density functionals erroneously predict the anthracene photodimerization reaction to be endothermic and that the product is unstable relative to non-interacting anthracene monomers.[2]

On the other hand, MP2 performs reasonably well for this reaction with much lower cost than CCSD(T), but it suffers from well-known problems in the treatment of van der Waals dispersion that cause it to overestimate the interaction energies. MP2D corrects this by replacing the uncoupled Hartree-Fock dispersion treatment inherently present in MP2 with an improved coupled Kohn-Sham treatment.[1] As shown in Figure S1, MP2D predicts energetics for the anthracene dimerization reaction that are much closer to the benchmark CCSD(T) ones than those from B86bPBE-XDM. Specifically, the gas-phase photodimer is predicted to be 13.4 kJ/mol more stable than the π-stacked monomers at the MP2D/CBS level, versus 14.1 kJ/mol with CCSD(T)/CBS.

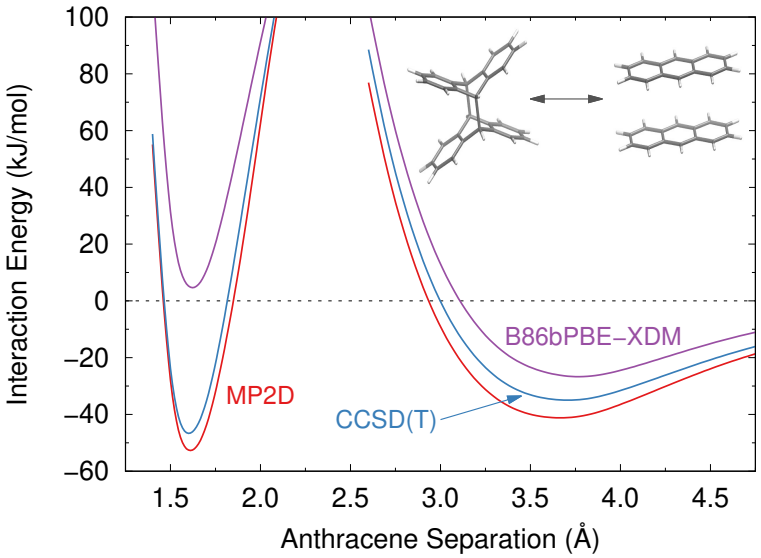

Figure S1: Potential energy curve for the anthracene dimer as a function of the distance between the central carbons. The photodimer occurs at short separations near 1.6 Å, while the non-covalent π dimer occurs around 3.6–3.8 Å.

S1.2 MP2D lattice energy refinement of 9TBAE lattice energies

From the anthracene data above, one expects the MP2D energetics to be much more reliable than the DFT ones. However, it is computationally impractical to employ MP2D directly to these crystals, even when using fragment methods such as the hybrid many-body interaction (HMBI) model developed by the author. The 9TBAE photodimer itself contains 78 atoms, and large basis sets are needed to describe the energetics accurately and avoid problems with intramolecular basis set superposition error. A full HMBI treatment would require computing the interactions between many different pairs of photodimers, at 156 atoms and nearly 7,000 basis functions per pair in the def2-QZVP basis.

However, the primary problem with the DFT results stems from the intramolecular description of the very short-range van der Waals interactions coupled with the large energy changes associated with small changes in the anthracene ring distortion and inter-ring separation in the photodimer. The longer-range intermolecular interactions between monomer or photodimer molecules should be well-described by B86bPBE-XDM. Therefore, the total energies of the crystals are approximated as the DFT energy of the entire crystal plus a correction for how the MP2D intramolecular energy differs from the DFT one,

$$E_{crystal} = E_{crystal}^{DFT} + \left(E_{intra}^{MP2D} - E_{intra}^{DFT}\right) \quad (1)$$

Table S1: Decomposition of the crystal energy into intra- and intermolecular contributions and the net energy after MP2D refinement (kJ/mol). All energies are reported relative to that of the SGD polymorph.

Crystal Structure	Intramolecular[a] B86bPBE-XDM	Intramolecular[a] MP2D	Intermolecular[b] B86bPBE-XDM	Total Energy[c]
SGD	0.0	0.0	0.0	0.0
SSRD *Pbca*	21.4	23.5	-10.2	13.3
SSRD $P2_1cn$	23.0	25.7	-11.9	13.8
SSRD *Aba*2	21.5	24.3	-10.1	14.2
SSRD $P2_12_12_1$	21.0	23.9	-9.6	14.2
SSRD *Pccn*	20.1	23.0	-8.7	14.4
SSRD $A2_122$	20.9	23.7	-9.2	14.4
SSRD $P2_1ca$	42.0	44.3	1.4	45.7
SSRD *Pcc*2	43.1	45.2	3.8	49.0

[a] Computed on isolated monomers at their crystalline geometries.

[b] Computed as $E_{inter}^{B86bPBE-XDM} = E_{crystal}^{B86bPBE-XDM} - E_{intra}^{B86bPBE-XDM}$

[c] Computed as $E_{total} = E_{intra}^{MP2D} + E_{inter}^{B86bPBE-XDM}$, which is equivalent to Eq 1.

The largest impact of this MP2D refinement will occur for the energetics of the monomer relative to the photodimer products. However, there will also be more subtle corrections arising from subtle differences in the anthracene photodimer product geometries across the different crystal structures. Indeed, Table 1 in the main paper shows that the MP2D energies

relative to the monomer crystal drop by ∼70-75 kJ/mol. MP2D has a smaller impact on the SSRD photodimer energies relative to the SGD, but it still increases the relative SSRD polymorph energy differences by ∼2-3 kJ/mol.

Further detailed is presented in Table S1, which decomposes the hybrid MP2D energies into the intra- and intermolecular portions. In addition to highlighting how MP2D alters the intramolecular energetics, one observes that although the SSRD polymorphs adopt conformations that are ∼23–26 kJ/mol higher in energy than the SGD polymorph, this is partially compensated (∼9–12 kJ/mol) for by the better intermolecular packing. Therefore, the total energy of the SSRD polymorphs is only ∼13–14 kJ/mol higher than the SGD.

S2 Examination of other relevant crystal systems

S2.1 Other polymorphs with exceptionally large lattice energy differences

Nyman and Day surveyed[3] the relative lattice energies for 508 polymorphic species (with 552 total pairwise polymorph energy comparisons) using a model that combined DFT treatment of the intramolecular conformation with a molecular mechanics treatment of the intermolecular interactions. They found eight polymorph pairs for which the difference in lattice energies between polymorphs exceeded 10 kJ/mol. Here, those eight cases were revisited here with periodic DFT, employing the same B86bPBE-XDM density functional as used for the 9TBAE system. A 50 Ry planewave cutoff was used, and the Monkhorst-Pack k-point mesh for each crystal was increased until the lattice energy differences converged to within 0.1 kJ/mol. All structures were optimized with periodic DFT starting from the experimental crystal structures.

Agreement between the experimental and optimized structures is generally good, as measured by the rmsd15 metric (root-mean square deviation in the non-hydrogen atom positions for a cluster of 15 molecules).[4] Most rmsd15 values lie between 0.1–0.2 Å, which is typical when comparing room-temperature experimental structures with predicted structures that neglect zero-point vibrations and thermal expansion. A few cases exhibit larger deviations. For JARXUV and JARXUV01, the ∼0.3 Å rmsd15 values stem from relatively subtle changes in angles about the flexible sp^3-hybridized carbons. For UKANOJ, the DFT calculations predict that the molecules are somewhat more planar, reducing the torsion angles between the central triazole and adjacent phenyl rings 45° to 27°.

Table S3 lists the Cambridge Structure Database (CSD) reference codes and lattice energy difference for those eight polymorph pairs as reported from Ref 3. The largest energy difference of 18.5 kJ/mol was found for 3,5-diphenyl-3-amino-1,2,4-triazole (UKANOJ/UKANOJ01). The energy differences decreased rapidly toward 10 kJ/mol from there. Periodic DFT refinement with B86bPBE-XDM decreases the lattice energy differences by 7.4 kJ/mol on average. In fact, only two systems, UKANOJ01/UKANOJ and N,N'-(*p*-phenylene)dibenzamide (PABZAM/PABZAM01) retain energy differences larger than 10 kJ/mol after the periodic DFT refinement.

The reasons for the large differences between the earlier calculations and the new ones here are not entirely clear, but they likely stem from limitations in the partial treatment

Table S2: Root-mean-square deviations (rmsd15, in Å) between the experimental and periodic B86bPBE-XDM optimized crystal structures.

Structure	rmsd15 (Å)	Structure	rmsd15 (Å)
UKANOJ01	0.199	UKANOJ	0.409
JARXUV	0.272	JARXUV01	0.319
PABZAM	0.136	PABZAM01	0.266
TRDMPP02	0.196	TRDMPP01	0.135
SLFNMB05	0.180	SLFNMB01	0.168
TINBIB	0.188	TINBIB01	0.280
UTORAX	0.158	UTORAX01	0.164
SUWMIG03	0.114	SUWMIG02	0.161

of molecular flexibility and/or deficiencies in the force field treatment of the intermolecular interactions in the earlier calculations. Subsequent refinements to the computational procedure in Ref 5 also reduced the lattice energy differences for a number of these polymorph pairs, bringing those results into closer agreement with the DFT results. In addition, several of these species have unusual electronic structure that may not be well described by the force field (extended π conjugation, sulfur atoms, etc). Although periodic DFT calculations were not performed for the full set of crystal structures of all 508 species in the original survey, these results further emphasize how rare lattice energy differences above 10 kJ/mol are.

Table S3: Comparison of lattice energy differences (kJ/mol) for the eight polymorph pairs with the largest energy differences from the survey of Nyman and Day[3] and follow-up study.[5] The crystal structures are indicated by their CSD RefCodes.

Stable Polymorph	Metastable Polymorph	Hybrid DFT+MM[3] (kJ/mol)	Refined DFT+MM[5] (kJ/mol)	Periodic B86bPBE-XDM (kJ/mol)
UKANOJ01	UKANOJ	18.5	—	15.9
JARXUV	JARXUV01	14.6	2.4	4.8
PABZAM	PABZAM01	13.7	10.6	10.5
TRDMPP02	TRDMPP01	13.4	4.9	2.0
SLFNMB05	SLFNMB01	12.4	2.6	3.5
TINBIB	TINBIB01	11.2	14.4	4.5
UTORAX	UTORAX01	11.1	—	6.3
SUWMIG03	SUWMIG02	10.4	10.5	-1.6

S2.2 Solid state synthetic memory in *p*-bromonitrosobenzene

Halasz and co-workers[6] have demonstrated that *p*-bromonitrosobenzene exhibits solid state synthetic memory, like 9TBAE. In particular, the monomer crystal structure **M1** (RefCode XAJPII) freshly obtained via sublimation differs from the polymorph **M2** (XAJPII01) generated via photodissociation of the crystalline dimer **D** (BNTBED01). Other dimer phases

have been reported[6] but are not considered here. **M1** is disordered, with the molecules arranged in layers but orientationally disordered in either a head-to-head or head-to-tail fashion. The head-to-head arrangement can dimerize readily due to having the adjacent NO groups in the crystal, whereas the head-to-tail form does not. Interestingly, the iodo-analog adopts an analogous crystal structure to **M1** which is ordered in the head-to-tail fashion, and it does not dimerize readily.[7] Experiments indicate that **M2** quickly returns to a dimeric phase at temperature above 170 K. A very recent study has also demonstrated interesting dynamics with remarkably large atomic displacements in solid state nitrosobenzene reactions.[8]

To model this system, periodic B86bPBE-XDM calculations were performed on the dimer crystal **D**, **M2**, and two "limiting" ordered forms of **M1** where the molecules were all arranged in head-to-head or head-to-tail arrangements (Figure S2). The dimer form is the most stable, with the other forms lying 27–36 kJ/mol higher. While the simplified treatment of the disordered **M1** form here is only approximate, the **M2** form is several kJ/mol less stable than the lowest lattice energy packing for **M1** (head-to-tail). In other words, the *p*-bromonitrosobenzene provides another example of solid-state synthetic memory, though the energy differences here are smaller than those found for the 9TBAE polymorphs.

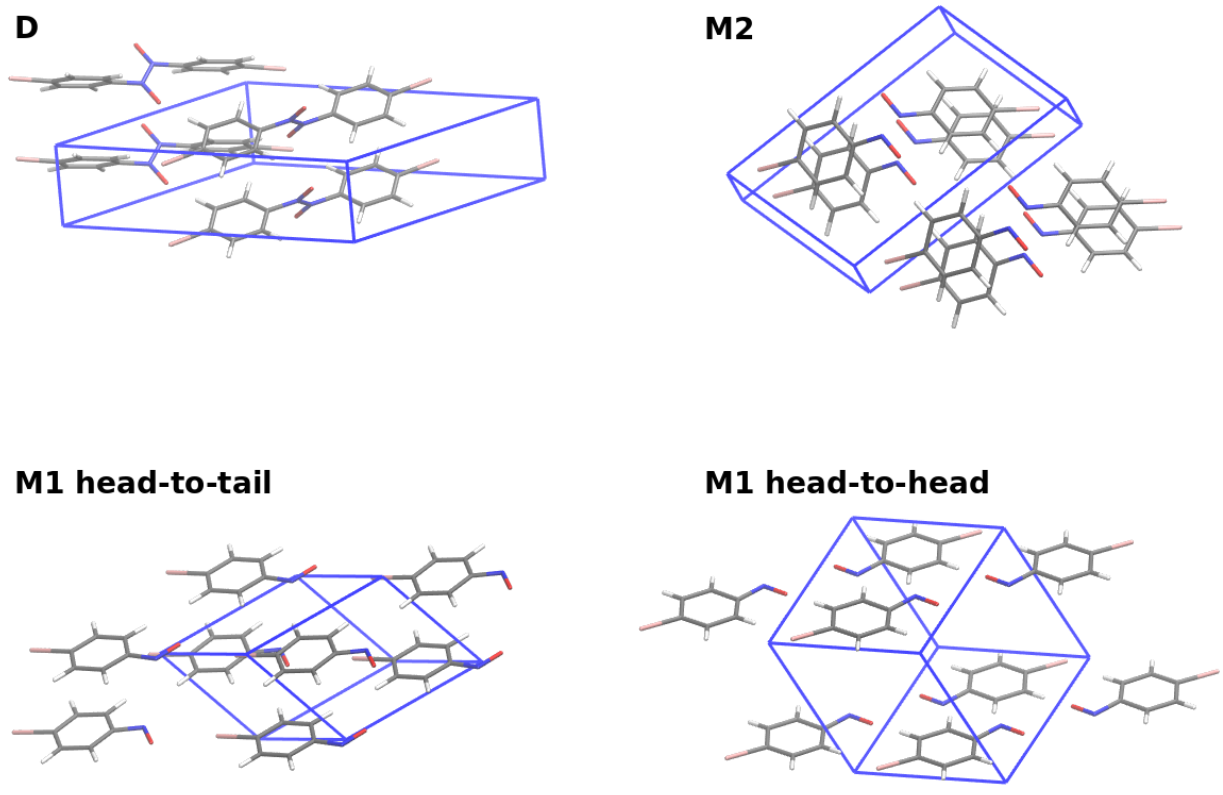

Figure S2: Optimized crystal structures for the *p*-bromonitrosobenzene dimer **D**, two ordered versions of monomer form **M1**, and monomer form **M2**.

Table S4: Relative energetics for the *p*-bromonitrosobenzene polymorphs.

Structure	Relative Energy (kJ/mol)
D	0.0
M1 head-to-tail	26.9
M2	31.3
M1 head-to-head	36.4

References

(1) Řezáč, J.; Greenwell, C.; Beran, G. J. O. Accurate non-covalent interactions via dispersion-corrected second-order Møller-Plesset perturbation theory. *J. Chem. Theory Comput.* **2018**, *14*, 4711–4721.

(2) Grimme, S.; Diedrich, C.; Korth, M. The Importance of Inter- and Intramolecular van der Waals Interactions in Organic Reactions: the Dimerization of Anthracene Revisited. *Angew. Chem. Int. Ed.* **2006**, *45*, 625–629.

(3) Nyman, J.; Day, G. M. Static and lattice vibrational energy differences between polymorphs. *CrystEngComm* **2015**, *17*, 5154–5165.

(4) Chisholm, J. A.; Motherwell, W. D. S. COMPACK: A program for identifying crystal structure similarity using distances. *J. Appl. Crystall.* **2005**, *38*, 228–231.

(5) Nyman, J.; Sheehan Pundyke, O.; Day, G. M. Accurate force fields and methods for modelling organic molecular crystals at finite temperatures. *Phys. Chem. Chem. Phys.* **2016**, *18*, 15828–15837.

(6) Halasz, I.; Mestrovic, E.; Cicak, H.; Mihalic, Z.; Vancik, H. Solid-state reaction mechanisms in monomer-dimer interconversions of p-bromonitrosobenzene. Single-crystal-to-single-crystal photodissociation and formation of new non-van der Waals close contacts. *J. Org. Chem.* **2005**, *70*, 8461–8467.

(7) Biljan, I.; Vancik, H. Aromatic C-Nitroso Compounds and Their Dimers: A Model for Probing the Reaction Mechanisms in Crystalline Molecular Solids. *Crystals* **2017**, *7*, 376.

(8) Rodenbough, P. P.; Karothu, D. P.; Gjorgjieva, T.; Commins, P.; Hara, H.; Naumov, P. Reversible Photolysis of Nitrosobenzene cis-Dimer Monitored In Situ by Single Crystal Photocrystallography. *Cryst. Growth Des.* **2018**, *18*, 1293–1296.